Aswan University Journal of Science and Technology Volume 3, issue 1, June 2023

Flexural Behaviour of Hybrid Bar Reinforced Concrete Beams (GFRP Bars with Steel Wires): An Experimental Study

Mamdouh Sayed Abdelbaqi[a,] *, Mohamed Ahmed Saifeldeen[b], Hossameldeen Mohamed[c], Omar Ahmed Farghal[d], Abd El Rahman Megahid Ahmed[e].

[a]Luxor Higher Institute of Engineering & Technology, Luxor 85834, Egypt.
[b]Faculty of Engineering, Aswan University, Egypt.
[c]Faculty of Engineering, Aswan University, Egypt.
[d]Faculty of Engineering, Assiut University, Egypt.
[e]Faculty of Engineering, Assiut University, Egypt

Abstract - Steel material is the most used material to be used with concrete due to its well-performance. Nevertheless, aggressive environmental conditions can lead to severe damage to steel bars due mostly to corrosion effects. Aside from that, steel production alerts the environment in many different ways. All these reasons promote engineers to define a new eco-friendly alternative for steel to be used in reinforced concrete structures. Thus, The use of fiber-reinforced polymer (FRP) as an alternative to steel reinforcement has become a popular research topic. One of the major drawbacks of using FRP is its low modulus of elasticity which might lead to a significant reduction in stiffness consequently, exceedance to deformation limit states. In this context, the concept of material hybridization is applied to increase the elastic modulus of GFRP bars by using steel in the RC beams. The FRP hybrid bar is designed and manufactured by combining two different materials, including fibres and steel and unsaturated polyester resins.This research presents an experimental study to investigate the flexural behaviour of concrete beams reinforced internally with hybrid reinforcement under static loading. A set of twenty reinforced concrete beams were monotonically tested under four-point bending. The beams with 2400 mm length, 150 mm width and 250 mm height were tested under four-point loads. Eight reinforced concrete beams underwent four-point bending monotonically. Crack pattern, Mode of Failure, cracking, ultimate load, mid span-deflection, primary reinforcement strain, and ductility index were examined. The GFRP area-to-concrete cross-section area ratio and hybridization ratio were examined.

Keywords: Hybrid Bar, Crack Pattern, Mode of Failure, Mid Span-deflection, GFRP, ultimate load, cracking load.

1. Introduction

The corrosion of reinforcement bar (reinforcing steel) is one of the primary factors contributing to the reduction in the service life of reinforced concrete constructions (RC). The physical issue of corrosion of steel bars is depicted in Figure 1 in [1]. The key problem for engineers is to develop affordable, sustainable, and eco-friendly building materials. It is imperative to find

Corresponding author E-mail: Mamdouhalngmy2@gmail.com

Received May 2, 2023 received in revised form May 19, 2023, accepted May 21, 2023.
(ASWJST 2023/ printed ISSN: 2735-3087 and on-line ISSN: 2735-3095) https://journals.aswu.edu.eg/stjournal

innovative building materials that can meet these needs. Over the past few decades, fiber-reinforced polymers (FRP) have been employed extensively as reinforcing materials [2]. FRP material was first pricey and only available in niche markets. FRP materials have been employed as an alternative to steel as reinforcing bars for concrete constructions for the past three decades [3]. FRP composites are more advantageous than steel since they are lightweight, noncorrosive, and have a high tensile strength. all of these reasons make the use of FRP as an affordable alternative to steel reinforcement. . Additionally, because they are nonconductive, they can be used in MRI facilities and other medical applications that are extremely sensitive to electromagnetic fields. Carbon fiber reinforced polymer (CFRP), Aramid fiber reinforced polymer (AFRP), glass fiber reinforced polymer (GFRP), and basalt fiber reinforced polymer (BFRP) are the FRP kinds that are most frequently utilized in infrastructure [3].

Fig. 1 Corrosion of steel bars.

FRP materials can be produced as sheets, plates, and wraps for uses such as strengthening existing structures, as bars and tendons for concrete reinforcement in new construction, or even as a structural element on its own. The low elasticity of FRP bars is a disadvantage since it causes more deformations, whereas steel bars result in higher ductility [4]. As illustrated in Fig. 2, [1, 5-8], hybrid bars are new kinds of reinforcement that are utilized as a good substitute for steel to strengthen a concrete structure and to address the disadvantages of FRP bars, such as cost and elastic modulus. The advantages and disadvantages of applying FRP and hybrid bars as reinforcement are compared in Table 1.

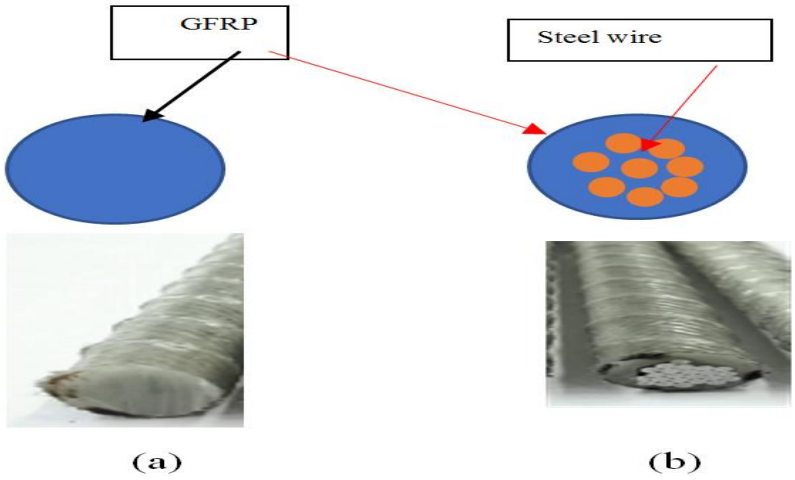

Fig. 2 Cross section types of "FRP Bar"; type (a) (GFRP bar); type (b) (GFRP with steel wires).

Table 1. Comparison between the use of FRP and use of hybrid bars in reinforced concrete structures.

The Advantages of FRP ACI (2015) [9].	The Disadvantages FRP ACI (2015) [9].	Advantage Hybrid Bars
High tensile strength.	brittle mode failure mechanism.	Low cost.
Corrosion-resistant	Low modulus of elasticity.	The fibres dose not corrode.
Nonmagnetic.	Premature exceedance of deformation limit state.	High modulus of elasticity.
High fatigue endurance (varies with type of reinforcing fibre).	High coefficient of thermal expansion perpendicular to the fibres, relative to concrete.	Light weight.
Lightweight (about 1/5 the weight of steel).	Inadequate thermal performance	Nonconductive.
Low thermal and electric conductivity (for glass and aramid fibres).	High material costs.	Nonmagnetic.
Adequate damping property.		High strength.
		Ductile failure.

2. Research Objectives:

This experimental investigation examines the flexural behavior of concrete beams reinforced with GFRP bars only or with hybrid bars in terms of cracking pattern and modes of failure, ultimate load, mid-span deflection, and GFRP and hybrid-bar tensile strain. Research sub-objectives are listed below.

3. Experimental Work Materials

Seven reinforced concrete beams with rectangular (15*25 cm) cross-section were tested. Four-point loading test is incrementally performed over a simple span of 2400 mm until reaching failure. By maintaining the shear-span-to-depth ratio at the level of 4.2, the flexural deformation mode is ensured to dominate the behaviour and other nonductile deformation modes are prevented. Also, the compression steel and stirrups were kept unchanged for all tested beams, where two bars with 8 mm diameter were used as compression steel and 8 mm mild steel bars at a spacing of 200 mm were used as stirrups.

The flexural behaviour of concrete beams reinforced with GFRP bars only or steel bars only and The possibility of using hybrid bars in concrete beams to investigate through experimental tests, the deflection behaviour of concrete beams reinforced with GFRP bars only, steel bars only or hybrid wire reinforcement, as well as the behaviour of deflection-related parameters. These involve bars strains, crack width and spacing. To test the FRP RC beams used in the study until failure to examine failure modes and the flexural behaviour. Investigate the flexural performance of hybrid bars reinforced of concrete beams experimentally. We tested beams with different reinforcement ratios of GFRP to steel wires in one. In order to achieve these objectives, three main groups (A), (B) and (C) were classified, group (A) was used as a reference, In group (B) the main parameter was the ratios of the area of GFRP steel bars (A_w) to area total area of hybrid bars (A_f+A_w). the main parameter in group (C) was the ratios of the area of GFRP bars (A_f) to the area of concrete cross section (A_c).

The mechanical properties of hybrid bars were tested according to Egyptian code (ECP208-2005) [10]. Table 2 shows the results. To improve concrete beam flexural behavior under static loads, RC beams reinforced with hybrid bars were tested. Eight 35-MPa reinforced concrete beams were made. These beams are tested under four-point loading bending over a basic span of 2400 mm. Their rectangular cross-section is 150 mm wide and 250 mm high. Flexural behavior requires 4.2 shear-span to depth ratio. All tested beams had two 8-mm top reinforcing bars. All beams included 200 mm-spaced 8 mm plain bars for shear reinforcement. Table 3 details the tested beams. Fig. 3 shows beam reinforcement details. Electrical strain gauges examined mid-span glass FRP, hybrid, and steel bar generated strains. These strain gauges were 15 mm long, 350 Ohms resistant, and 2.04 gauges factor. Fig. 4 shows the strain gauges attached to the bottom surface of primary reinforcement at mid span. All beams were examined after 28 days. Cranes installed the beams on the test equipment. The data recording system (Fig. 6) coupled the LVDTs and crack width measurement device (Fig. 5 b and c). Before testing, instruments were checked and zeroed. The static load was applied in 0.4-ton increments until cracking, then continuously until failure.

Table 2. Properties of tested bars

Specimen type	Nominal diameter (mm)	Actual diameter (mm)	Yield tensile strength or proof strength (Mpa)	Ultimate tensile strength (Mpa)	Elastic Modulus of Elasticity (GPa)	Modules of Toughness (MPa)
Steel (B240C-P) (mm)	8	7.9	248	355	195	11.1
GFRP	16	16	------	1103	48.75	14.09
hybrid 50%Steel	8	8.2	538.68	804	118	10.47
hybrid 50%Steel	16	16.1	792.677	1183.1	145	18.22
hybrid (G+D-W) 25%Steel	10	9.8	522.6	780	48.75	10.83
hybrid (G+D-W) 50%Steel	10	10.07	586.25	875	127	13.97
hybrid (G+D-W) 75%Steel	10	10	703.5	1050	180	12.199

Table 3. The details of the tested beams.

Group	Beam NO	BOTTOM REINF.	$(A_f/A_c)\%$	$A_w / (A_f + A_w)$	System of tension reinforcement
A	S1	2 Ø 8	0	------	Steel
	G1	2 Ø 16	1.19		GFRP
	W	2Ø10	0		Hybrid bars
B	W1	2Ø10	------	0.25	Hybrid bars
	W2	2Ø10		0.50	
	W3	2Ø10		0.75	
C	W4	2Ø 8	------	0.25	Hybrid bars
	W5	2Ø10		0.50	
	W6	2Ø16		0.75	

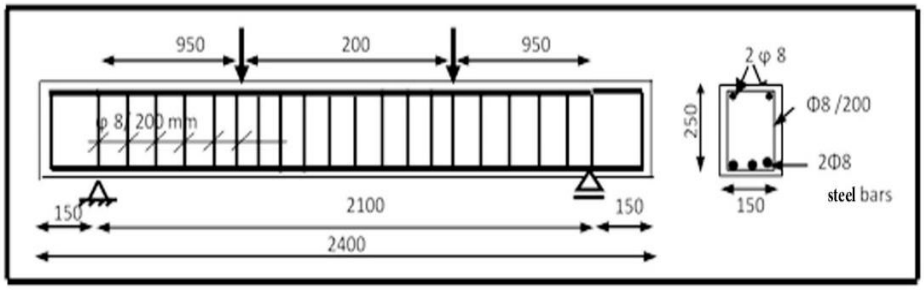

Fig. 3 Tesed Beams description S1.

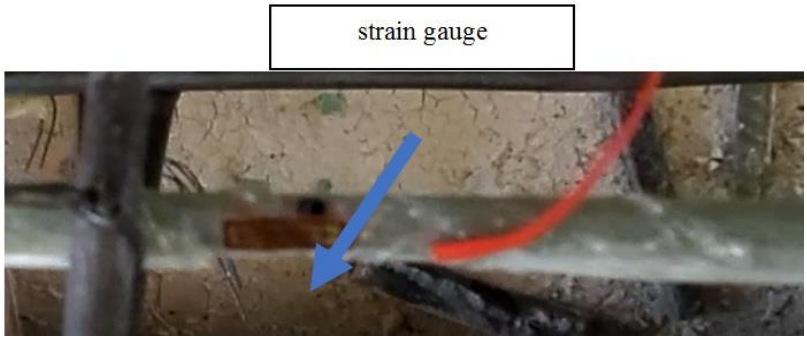

Fig. 4 Strain Gauge Installation

4. Testing Machine, Setup And Procedure

All prepared beams were tested at age of 28 days under a static monotonic test(Fig. 5 (a)) . The load is applied using a loading cell with an increment of 0.5 tons until reaching failure using the testing setup shown in Figure 3.45. Each increment is applied for two minutes before the start of the next loading increment. After each increment, the crack widths are measured using a crack width device installed within the testing setup (Fig. 5 (C)). Also, the stain is recorded using strain gauges. The stain gauges were connected to the data acquisition system prior to loading. Strain gauges at the mid-span with a 350 Ohms resistance, 2.04 gauges factor and a

length of 15 mm are used to measure reinforcement strain. In another hand, strains in concrete at the top of the tested beam were recorded using a strain gauge with a resistance of 120 ohms and length of 67 mm. Also, the mid-span deflection was recorded using a linear variable differential transducer (LVDT) (Fig. 5 (b)) connected to the data logger system (Fig. 6).

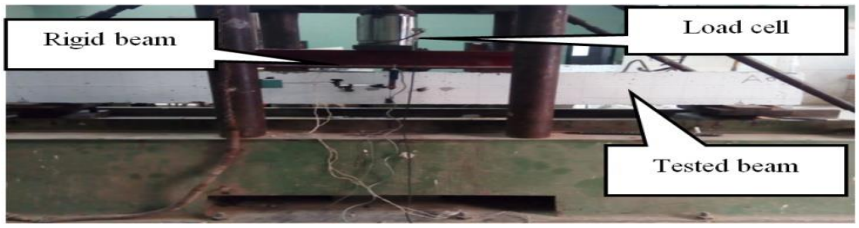

Fig. 5-A Set up of tested beams

Fig. 5-B LVDT

Fig. 5-c Crck width measurement Device

Fig. 5 Experimental tools

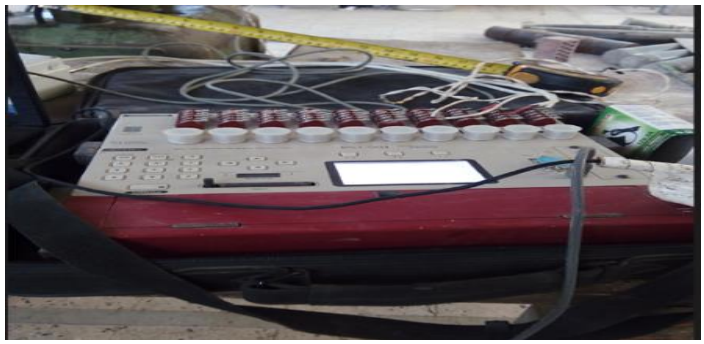

Fig. 6 Data loggers system

5. Test Results and Discussion

5.1 Crack Patterns and Mode of Failure

Crack propagation was seen and magnified for each beam investigated. All beams had similar cracks on both sides. The bottom flexural moment zone cracks started at low load. The first crack reached half the beam depth. Cracks spread higher as load increased. Later, new cracks formed along the beam's bottom and propagated toward the load. Cracks varied with load. All tested beams had the following failure modes:

For Group A (S1,G1 and W)

For beams of (G1) with GFRP bars, the number of cracks at failure was noticed to be fewer than that in reference beam (S1) and (w) which having steel bars only and hybrid wires bar respectively. The cracks height and width in beams of (G1) was more than the reference beams (S1) and (W) . This is due to the low modulus of elasticity of GFRP bars than steel bars or hybrid wires bars, see Fig. 7 to 9.

For Group B (W1, W2, W3)

It is observed that the number of cracks in hybrid beams W3 and W2 is more than that in the beams W3. This mainly due to the ratio of A_f / (A_f +A_w) in W3 and W2 is less than that in beams W1. Also, for this reason the number of cracks in beam W3 are more than that in beam G1. Also, the crack widths in beams W1 and W2 were less than that in beam W3. The modes of failure in beams W2 were flexural failure while in beam W1 was flexure - shear compression failure. Flexural with bond failure occurred in W3. Is reinforced with 25% glass and 75 wire, this makes the wire more controllable in the mode of failure and the design under reinforcement, Increasing the wire ratio (from 25% to 75%) effect on improving the cracking behavior, as shown from Fig. 10 to 12.

For Group C (W4, W5 and W6)

The effect of the reinforcement Ratio of hybrid FRP bars (ρ_w%) on the crack patterns for beams (W4, W5, and W6) in group C are shown in Fig. 9 to 14. For an increase in the reinforcement ratio of FRP, bars (ρ_w%) from 0.298% to 1.19 the effect of Reinforcement Ratio of FRP bars (ρ_w%) showed to have minimal influence on the behaviour of cracks. the cracks propagated slowly towards the point of load applications. the number of cracks is increased (from 10 to 17) cracks. The average spacing between cracks was decreased (from 33 to 18.3) cm. the average crack width was decreased (from 2 to 1.9 mm) Furthermore, there was no appearance of the lower horizontal cracks. Beam (W4) with low (ρ_w%) have wide, long cracks in contrast to the shorter, narrow cracks found in beams with higher (ρ_w%) .

The modes of failure in beams W4, W5 and W6 were flexural failure while in beam W4 was flexural with rupture in hybrid bar. Flexural with bond failure occurred in W5. The final failure mode was changed from flexural compression in beam W4 to flexural shear with bond failure accompanied by splitting failure in beam W6 caused by the dowel action and due to increasing in the ultimate load as shown from Fig. 9 to 14.

Fig. 7 Pattern of cracks of beam (S1).

Fig. 8 Pattern of cracks of beam (G1).

Fig. 9 Pattern of cracks of beam (W).

Fig. 10 Pattern of cracks of beam (W1).

Fig. 11 Pattern of cracks of beam (W2).

Fig. 12Pattern of cracks of beam (W3).

Fig. 13 Pattern of cracks of beam (W4).

Fig. 14 Pattern of cracks of beam (W5).

Fig. 15 Pattern of cracks of beam (W6).

5.2 Cracking and Ultimate Loads

In comparison to beam group (A) reinforced with GFRP bars only or hybrid wires bars, the cracking load for concrete beam (S1) provided with steel bars only is larger. In terms of cracking load, groups (B) and (C) are nearly identical to group (A). The following differences across groups can be seen in the increase in cracking and ultimate load: -

For Group A (S1, G1 and W)

The ultimate failure load for beams reinforced with steel reinforcement is higher than that of GFRP beams, as illustrated in Fig. 15. The results obtained are consistent with those previously reported by [11]. This might be explained by the GFRP bars' low elastic modulus. When GFRP-reinforced beams were compared to beams with conventional steel reinforcement, it was discovered that the crack initiation load was lower in the GFRP-reinforced beams due to the reduced modulus of elasticity of GFRP bars. The acquired result supports the earlier finding made public by [12].

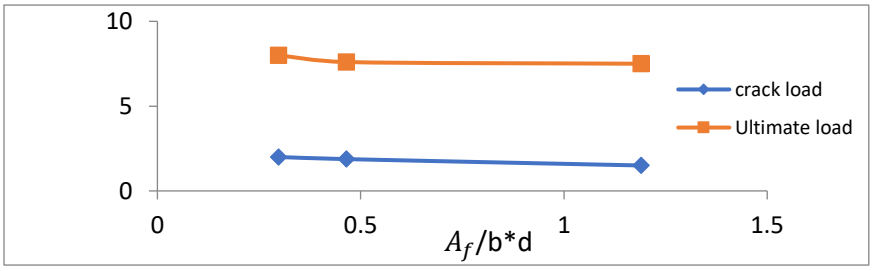

Fig. 16 Different types of reinforcement on the ultimate and crack loads.

For Group B (W1, W2 and W3)

The impact of the hybrid bars' A_f / (A_f +A_w) ratio on cracking and ultimate load for the tested beams is depicted in Fig. 17. These numbers make it clear that the final load decreases when the A_f / (A_f +A_w) ratio rises. However, the modification in the A_f / (A_f +A_w) ratio has not had an impact on the cracking load.

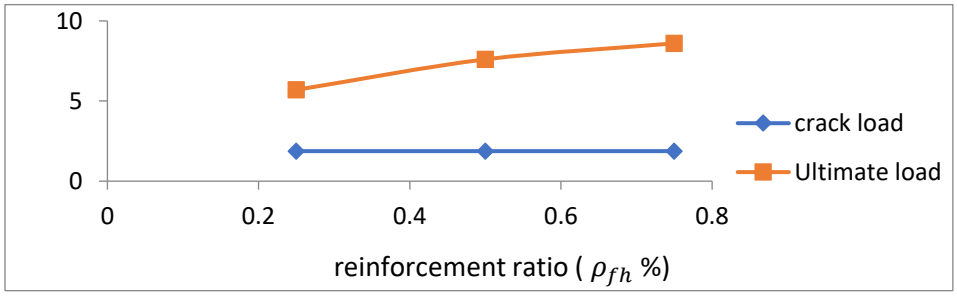

Fig. 17 Effect of $A_f/ (A_f + A_w)$ ratio on cracking and ultimate load for beams group B.

For Group C (W4, W5 and W6)

The final flexural capacity is affected by different reinforcement ratios, as shown in Figure 4.38 and Table 4.11. The reinforcing ratio of FRP bars (ρ_w%) for beams (W4, W5 and W6) was 0.298, 0.465, and 1.19, respectively.

The reinforcement ratio increased by about 299.3% (from 0.298 to 1.19%), which resulted in an increase in the ultimate flexural strength of 185.7%. This improvement in flexural strength was brought on by the beam's enhanced bearing capacity. When the reinforcement ratio was raised, the number of cracks increased but their width reduced. The area of the aggregate interlock and the contribution of the un cracked concrete are increased by expanding the concrete compression zone. On the other hand, a high percentage of hybrid FRP bars reinforcement accelerates the dowel action failure which prevents the beam to reach its full ultimate flexural capacity.

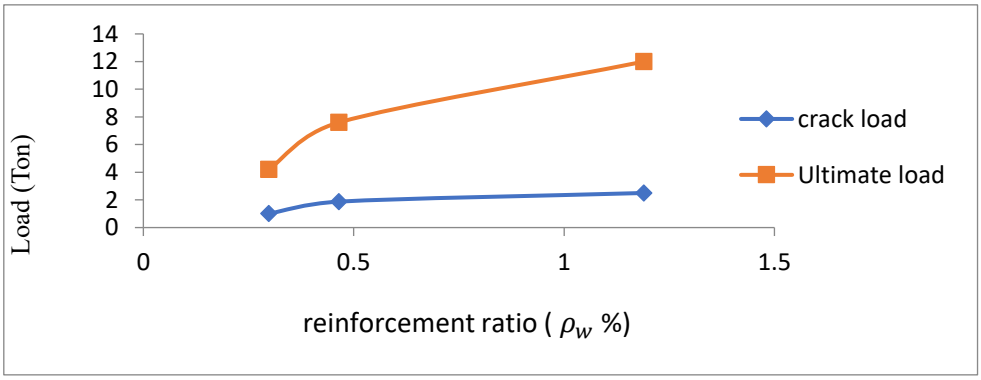

Fig. 18 Reinforcement ratio (ρ_w%) effect on ultimate and crack loads.

5.3 Mid-Span Deflection

The relation between the applied load and the measured mid-span deflection is illustrated from Figures 19 to 21, for different tested beams. Generally, through these figures, it is obvious that the initial part of the curves was linear for all beams. At the end of the linear phase, the beams began to crack. Also, in these figures, it can be seen that the deflection at failure in groups B and group C was slightly larger than that in beam S1 (control).

For Group A (S1, G1 and W)

The increase in deflection after first cracking up to (50%) of the ultimate load for beam G1 (3G) which was reinforced with GFRP bars only was 450% more than that for beam S1 which was reinforced with steel bars only as shown in Figure 19. The obtained results showed a similar trend as was observed in a previous work by [13].

For group B (W1, W2 and W3)

Fig. 20 present the load- mid span deflection for beams W (1,2 and 3), It is observed that by increasing the ratio of the A_f / (A_f +A_w) ratio, this increased the deflection in the beam's hybrid bars because of the low modules of elasticity of the fibre compared to the steel wires.

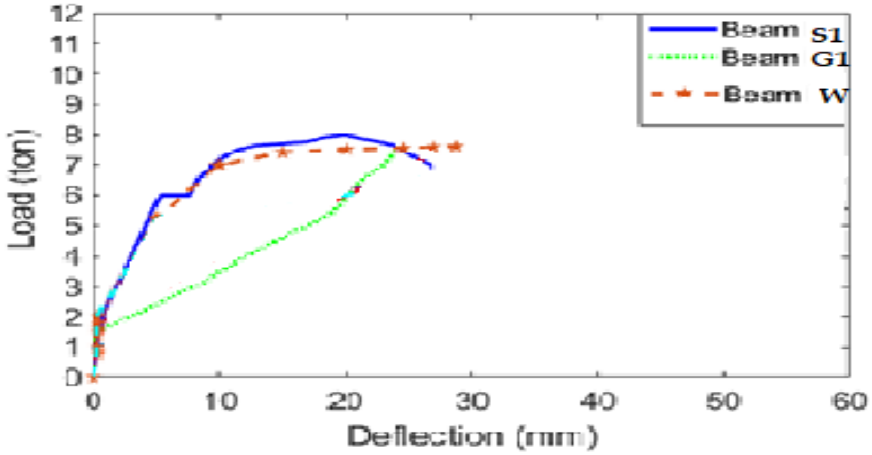

Fig. 19 Load mid-span deflection curves for group A.

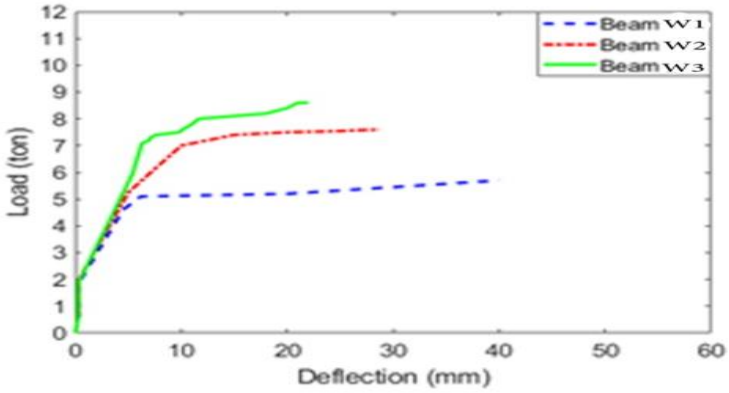

Fig. 20Load mid-span deflection curves for hybrid beams (W1, W2 and W3

For group C (W4, W5 and W6)

Series C beams were given the designations W4, W5 and W6. The percentage of tension reinforcement (A_f /A_c %) was the parameter that this series of studies focused on. Two hybrid FRP bars with bottom ribs that were 8, 10, and 16 mm in diameter were used to reinforce these beams. These beams' concrete had a compressive strength of about 37 MPa.

Results for deflection in beams (W4, W5 and W6) with varying primary reinforcement were plotted in Figure 21 as applied flexural capacity load-deflection curves. All beams displayed linear flexural load-deflection behavior from the first loading stage to the breaking load. The flexural load-deflection curve diverged and got a little flatter after this point.

When the applied load exceeds the cracking load and causes a drop in stiffness, cracking occurs at the maximum moment zone with increasing applied force. There were bigger deflection values in beam (W4) than in beams (W5 and W6) at any level of loading, it was observed. This is brought on by the hybrid bars' low reinforcement ratio in beam (W4) when compared to beams

(W5 and W6).When (ρ_w%) rose to 1.19% in beam W6, the reduction in mid-span deflection was about 90% at the flexural force equivalent to 4.2 tons (ultimate flexural load for beam W4).

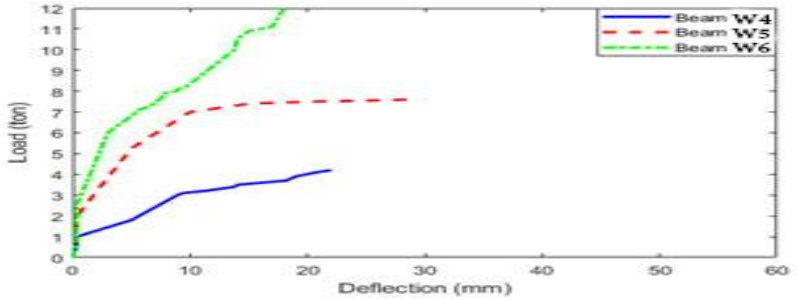

Fig. 21Load mid-span deflection curves for hybrid beams (W3, W4 and W5).

5.3 Ductility and Toughness

Based on the measurement of the mid-span deflection during failure and cracking, the ductility of reinforced concrete beams can be determined. The area under the load-deflection curve, which serves as a proxy for the energy absorption capacity, can also be used to quantify toughness. The ratio between the maximum deflection [Δ_{max}] and the deflection corresponding to the cracking load [Δ_{cr}] was used to calculate the displacement ductility index [μ_D] that was taken into consideration. The area under the load-deflection graph for the RC beams under static loading was calculated in order to establish the total energy absorption capacity (E_{abs}).

The total energy absorption capacity can be used to gauge how tough reinforced concrete beams are. Fig. 22 shows how the hybrid bar ratio A_f / (A_f +A_w) affects the displacement ductility index for these reinforced beams. These figures show that for beams with the same total area of reinforcement, the ductility index increased when the A_f / (A_f +A_w) ratio decreased. Fig. 22

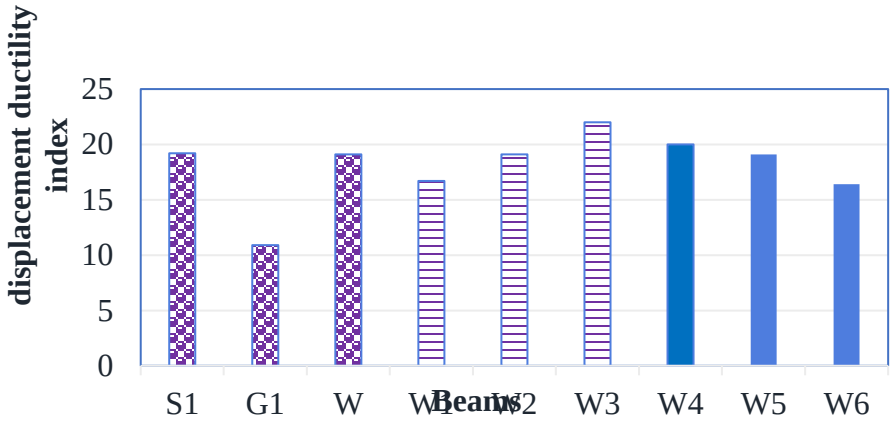

demonstrated that for group (C), the ductility index rose as the ratio of tensile reinforcement decreased. Additionally demonstrates that group B has better ductility than group A.

Fig. 22Ductility for beams

Fig. 22, According to the experimental findings, steel beams have a greater capacity to absorb energy than FRP beams and nearly identical hybrid FRP beams in group (A).

With an increase in the hybridization ratio (ρ_{fh}), there is a comparable decrease in group (B). Additionally, in Group (C), the amount of energy absorption decreases as the reinforcement ratio (ρ_w %) rises. This is due to the fact that as the hybridization ratio (ρ_w %) grows, the area under the deflection curve decreases.

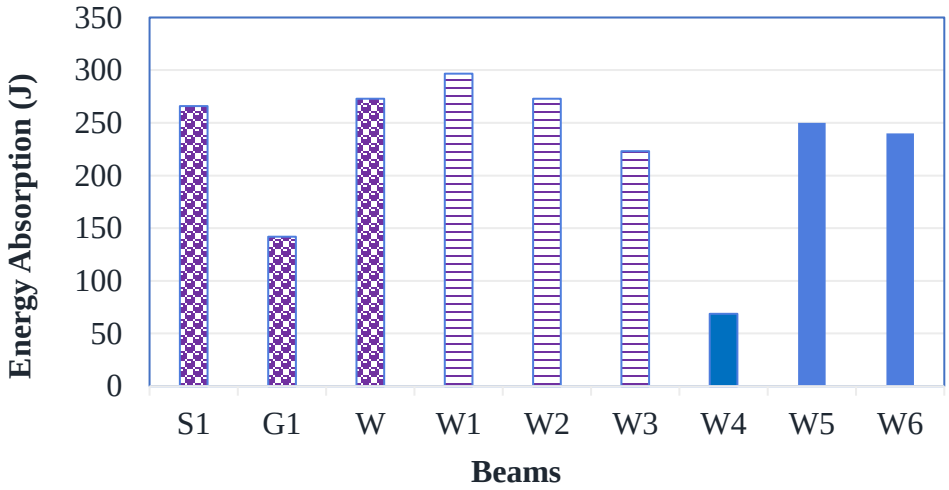

Fig. 23 Energy absorption capacity for beams.

5.4 Induced strain

For beams tested under static load, the major longitudinal reinforcement (steel, glass FRP bars, and hybrid bars) tensile strain was measured at mid span. Figs. 23,24 and 25 illustrate the measured values against applied load from zero loading to failure.

For Group A (S1, G1 and W)

It is clear from Fig. 23 that the strain rise following the first crack for the glass FRP reinforced concrete beam G1 is greater than for the beams S1 and W, which were reinforced with steel bars only and hybrid bars only, respectively. This indicates that following the initial crack, the deformation of GFRP concrete beams expands rapidly. It is obvious from this figure that beam G1 recorded a larger strain in GFRP bars after the cracking stage and at any load level. This is caused on by GFRP's reduced elasticity modulus, The load strain relationship increased linearly up to failure as the applied load increased.

For Group B (W1, W2 and W3)

Fig. 25 depicts the load strain curve for hybrid bars in beams W1, W2, and W3. The load strain curves were found to be linear up until cracking. Following that, the curves' trend is semi-linear all the way to failure. This results from the interaction between steel wires and glass fibers. Any load level saw an increase in strain value due to an increase in the A_f / (A_f +A_w) ratio in bar. For instance, the measured strain values for a beam made of 75% glass and 25% steel wires were higher than those for hybrid bars made of 25% glass and 75% steel wires. This is because fiber has a lower modulus of elasticity than steel. In comparison to GFRP beams, the hybrid bar bears higher ultimate weights and less strain.

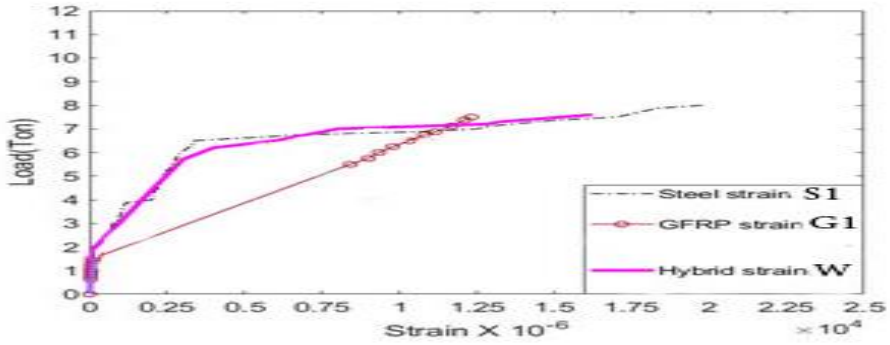

Fig. 25 Reinforcement Strain Relationships on Beams (W1, W2 and W3).

For Group C (W4, W5 and W6)

Fig. 26 depicts the load strain curve for hybrid bars in beams W1, W2, and W3. The ultimate strain was smaller than the strain in the reinforcement at failure in beams reinforced with FRP bars. The majority of the beams collapsed when the reinforcing in beam W4 reached its absolute limit of strength and ruptured.

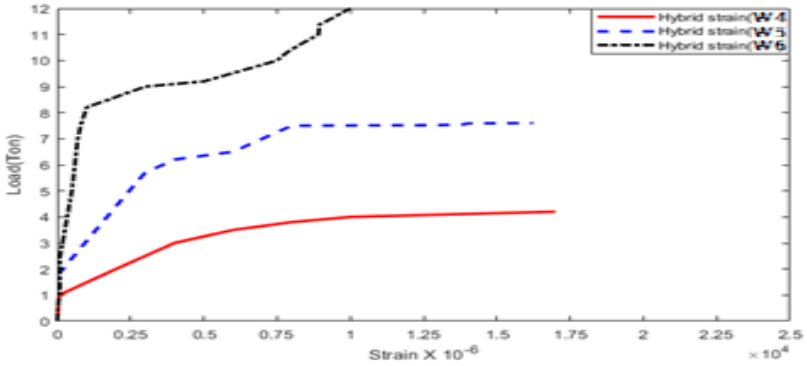

Fig. 26 Reinforcement Strain Relationships on Beams (W4, W5 and W6).

5.5 Crack Spacing

Fig. 26 displays the average crack spacing for each element in the constant flexure zone. Cracks did develop beneath or very near the two loading blocks in each of the cases. In order to calculate the average spacing, divide the length of the constant flexure zone by the number of cracks there, minus one. Due to the inadequate bond between GFRP and concrete, the fracture spacing in beams reinforced with GFRP bars exclusively is higher than that in beams reinforced with hybrid bars. In accordance with Figure 26, the average crack spacing in Groups B and C is approximately 1.5 and 1.4 times, respectively, that of Beam A0's minimum crack spacing.

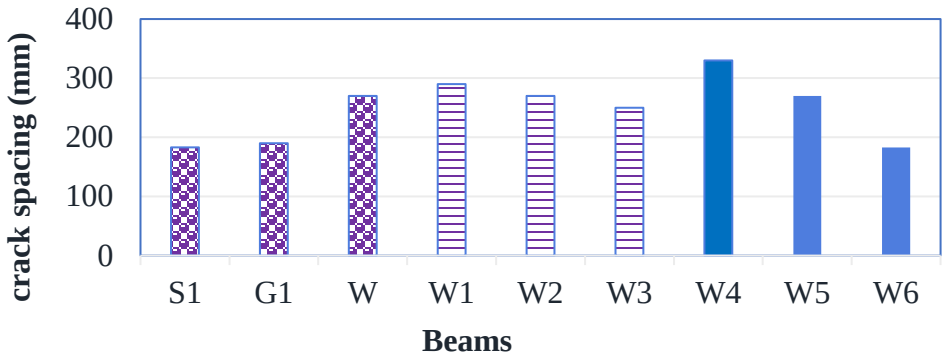

Fig. 27Average spacing of the cracks in the constant flexure zone

5.6 Crack Width.

The load-crack width relationship is depicted in Fig. 28. The crack widths were minimized by raising the steel reinforcement ratio. At any load, crack widths in FRP-reinforced members are anticipated to be greater than those in steel- or hybrid-reinforced RC beams because most FRP bars have a lower modulus of elasticity than steel. Before the concrete began to crack, all specimens showed elastic properties. At constant moment regions, short and fine flexural cracks started to form as the vertical load increased. As vertical loads increased, fine vertical cracks developed longer and wider, and a few new cracks appeared at constant moment and bending shear zones. Steel-RC beams had the smallest crack widths because they had higher reinforcing axial stiffness (E_s*A_s) than FRP-RC beams. GFRP-RC beams had 2.4 times the average crack width of steel-RC beams at the yield load. Steel bars' higher modulus of elasticity than GFRP bars predicted these

results. The beams reinforced with GFRP or hybrid bars had bigger cracks at any load than the control beam reinforced with steel.

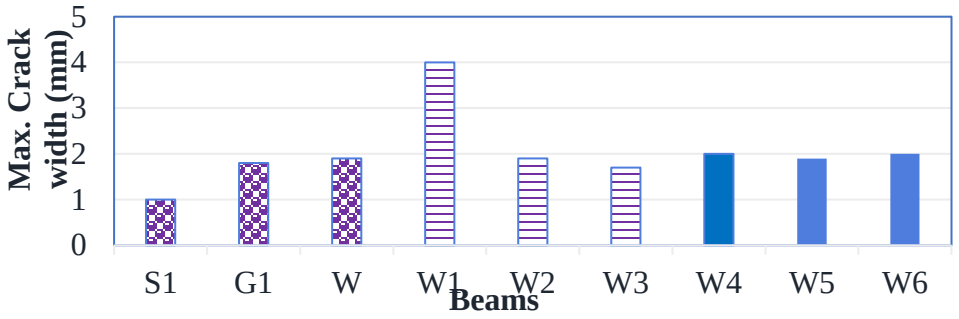

Fig. 28 Load vs. mid-span crack width for beams having the same tensile force of the main reinforcement.

6. Conclusions

The main results can be drawn from the studies done on beams strengthened longitudinally with hybrid bars and the predicted results: -

1) In hybrid reinforced beams, it is acceptable to be designed as over reinforcement beams if the ratio of A_f / (A_f +A_w) ≥ 50%.
2) Steel wire content in hybrid beams primarily controls the cracks' width. The width of the cracks reduces as the ratio of steel wires increases.
3) At any load, the hybrid beams' crack width is less than the GFRP beams' crack width.
4) The number of cracks decreased and the distance between them increased as the A_f / (A_f +A_w) ratio increased.
5) When determining the improvement in the flexural behavior of concrete beams with hybrid bars, using the A_f / (A_f +A_w) ratio provides a suitable parameter.
6) In hybrid bars reinforced beams, the moment capacities were reduced by decreasing the A_f / (A_f +A_w) ratio.
7) When compared to beams reinforced with hybrid bars, GFRP reinforced beams simply show greater deflection. This is brought on by the GFRP bars' lower elasticity modulus.
8) The mid span deflection in group B beams significantly decreased as the proportion of steel wires increased in hybrid beams from zero to 75%.
9) Less deflections were seen in hybrid reinforced beams compared to GFRP bar-only reinforced beams at the same load level.
10) In comparison to GFRP beams, hybrid beams have greater ductility indices. This is because one bar has steel wires and glass fibers.
11) In hybrid reinforced beams, increasing ductility was achieved by replacing some of the GFRP bars with steel wire.
12) Since the hybrid beam in (Group C) has a higher load capacity, bond shear failure, like in the equivalent in (W6), has replaced concrete crushing and rupture flexural failure as the mode of

failure.

13) With increased various reinforcement ratios (ρ_f %) (1.0, 1.875, and 2.5) and an increase in ultimate load, respectively, the cracking load of all beams in Group (C) had a negligible effect.
14) With an increase in the reinforcement ratio (ρ_w %) in Group (C), such as W5 and W6, the amount of energy absorption decreases in the higher reinforcement ratio.
15) At any loading level, the deflection values in beam (W4) were higher than those in beams (W5 and W6). This is because hybrid bars in beam (W4) have a lower reinforcement ratio than those in beams (W5 and W6).

References

[1] K. Park, H. Kim, Y. You, S. Lee, and D. Seo, (2013), "Hybrid FRP Reinforcing Bars for Concrete Structures," 4th Asia-Pacific Conf. FRP Struct., no. December, Melbourne, Australia, p. 6.

[2] Korea Institute of Construction Technology (KICT). (2012), "A Proposal for The Development of a Hybrid FRP Reinforcing Bar for Waterfront Structures," in KICT Report 2012-050. Korea.

[3] R. Fico, (2008), "Limit States Design of Concrete Structures Reinforced with FRP Bars.," Univ. Naples Federico II, PH. D. Thesis, p. 167.

[4] J. R. Yost, S. P. Gross, and D. W. Dinehart, (2001), "Shear strength of normal strength concrete beams reinforced with deformed GFRP bars," J. Compos. Constr., vol. 5, no. November, pp. 268–275.

[5] Dong-Woo Seo, Ki-Tae Park, Young-Jun You, and Sang-Yoon Lee (2016), "Experimental Investigation for Tensile Performance of GFRP-Steel Hybridized Rebar" Adv. Mater. Sci. Eng., vol. 2016, pp. 1–12, 2016.

[6] D.-W. Seo, K.-T. Park, Y.-J. You, and H.-Y. Kim (2013), "Enhancement in Elastic Modulus of GFRP Bars by Material Hybridization," Engineering, vol. 05, no. 11, pp. 865–869.

[7] J.-H. Hwang, D.-W. Seo, K.-T. Park, and Y.-J. You (2014)., "Experimental Study on the Mechanical Properties of FRP Bars by Hybridizing with Steel Wires," Engineering, vol. 06, no. 07, pp. 365–373.

[8] Seo, D. W., Park, K. T., You, Y. J., & Hwang, J. H. (2014). Evaluation for tensile performance of recently developed FRP hybrid bars. International Journal of Emerging Technology and Advanced Engineering, 4 (6), 631-637.

[9] ACI Committee 440.1 R-15, (2015), "Guide for the Design and Construction of Structural Concrete Reinforced with FRP Bars," Am. Concr. Inst., p. 88.

[10] Egyptian Code of Practice for Design and Construction for FRP Reinforced Concrete Structures, (ECP208-2005), Housing and Building National Research Center, Giza, Egypt.

[11] R. K. Abd-elwahab and A. S. Elamary, (2015), "Ductile Failure of Concrete Beam Reinforced with GFRP," Int. J. Emerg. Technol. Adv. Eng., vol. 5, no. 5, pp. 60–70.

[12] S. Y. Roja, P. Gandhi, D. M. Pukazhendhi, and R. Elangovan (2014), "Studies on Flexural Behaviour of Concrete Beams Reinforced with GFRP Bars," Int. Conf. Emerg. Trends Sci. Eng. Technol.

[13] A. El-nemr, E. Ahmed, and B. Benmokrane, (2011), "Instantaneous Deflection of Slender Concrete Beams Reinforced with GFRP Bars," 2nd Int. Eng. Mech. Mater. Spec. Conf. (CSCE), Ottawa, Ontario, June, pp. 1–10.